
Discovering Parametric Activation Functions

Garrett Bingham

The University of Texas at Austin and
Cognizant Technology Solutions
San Francisco, CA 94111
bingham@cs.utexas.edu

Risto Miikkulainen

The University of Texas at Austin and
Cognizant Technology Solutions
San Francisco, CA 94111
risto@cs.utexas.edu

Abstract

Recent studies have shown that the choice of activation function can significantly affect the performance of deep learning networks. However, the benefits of novel activation functions have been inconsistent and task-dependent, and therefore the rectified linear unit (ReLU) is still the most commonly used. This paper proposes a technique for customizing activation functions automatically, resulting in reliable improvements in performance. Evolutionary search is used to discover the general form of the function, and gradient descent to optimize its parameters for different parts of the network and over the learning process. Experiments with three different neural network architectures on the CIFAR-100 image classification dataset show that this approach is effective. It discovers different activation functions for different architectures, and consistently improves accuracy over ReLU and other recently proposed activation functions by significant margins. The approach can therefore be used as an automated optimization step in applying deep learning to new tasks.

1 Introduction

The Rectified Linear Unit ($\text{ReLU}(x) = \max\{x, 0\}$) is the most commonly-used activation function in modern deep learning architectures [22]. When introduced, it offered substantial improvements over the previously popular tanh and sigmoid activation functions. Because ReLU is unbounded as $x \rightarrow \infty$, it is less susceptible to vanishing gradients than tanh and sigmoid are. It is also simple to calculate, which leads to faster training times.

Activation function design continues to be an active area of research, and a number of novel activation functions have been introduced since ReLU, each with different properties [23]. In certain settings, these novel activation functions lead to substantial improvements in accuracy over ReLU, but the gains are often inconsistent across tasks. Because of this inconsistency, ReLU is still the most commonly used: it is reliable, even though it may be suboptimal.

The improvements and inconsistencies are due to a gradually evolving understanding of what makes an activation function effective. For example, Leaky ReLU [20] allows a small amount of gradient information to flow when the input is negative. It was introduced to prevent ReLU from creating dead neurons, i.e. those that are stuck at always outputting zero. On the other hand, the ELU activation function [4] contains a negative saturation regime to control the forward propagated variance. These two very different activation functions have seemingly contradicting properties, yet each has proven more effective than ReLU in various tasks.

There are also often complex interactions between an activation function and other neural network design choices, adding to the difficulty of selecting an appropriate activation function for a given task. For example, Ramachandran et al. [24] warned that the scale parameter in batch normalization [15] should be set when training with Swish; Hendrycks and Gimpel [13] suggested using an optimizer

Table 1: Operator search space. For ELU, $\alpha = 1$. For SELU, $\lambda = 1.05070098$ and $\alpha = 1.67326324$. The unary operators `bessel_i0e` and `bessel_i1e` are the exponentially scaled modified Bessel functions of order 0 and 1, respectively.

	Unary		Binary
0	<code>erf(x)</code>	$\sigma(x) = (1 + e^{-x})^{-1}$	$x_1 + x_2$
1	<code>erfc(x)</code>	$\log(\sigma(x)) = \log((1 + e^{-x})^{-1})$	$x_1 - x_2$
x	<code>sinh(x)</code>	<code>ReLU(x) = max{x, 0}</code>	$x_1 \cdot x_2$
$-x$	<code>cosh(x)</code>	<code>Softplus(x) = log(e^x + 1)</code>	x_1/x_2
$ x $	<code>tanh(x)</code>	<code>Softsign(x) = x/(x + 1)</code>	$x_1^{x_2}$
x^{-1}	<code>arcsinh(x)</code>	<code>HardSigmoid(x) = max{0, min{1, 0.2x + 0.5}}</code>	$\max\{x_1, x_2\}$
x^2	<code>arctanh(x)</code>	<code>ELU(x) = x if x > 0 else $\alpha(e^x - 1)$ [4]</code>	$\min\{x_1, x_2\}$
e^x	<code>bessel_i0e(x)</code>	<code>SELU(x) = λx if $x > 0$ else $\lambda\alpha(e^x - 1)$ [16]</code>	
$e^x - 1$	<code>bessel_i1e(x)</code>	<code>Swish(x) = $x \cdot \sigma(x)$ [24, 6]</code>	

with momentum when using GELU; Klambauer et al. [16] introduced a modification of dropout [14] called alpha dropout to be used with SELU.

These results suggest that significant gains are possible by designing the activation function properly for a network and task, but that it is difficult to do so manually. This paper presents an approach to automatic activation function design. In contrast with previous studies [3, 24, 19, 2], this paper focuses on automatically discovering activation functions which are parametric. Evolution discovers the general form of the function, while gradient descent optimizes the parameters of the function during training. The approach, called Parametric Activation functions Generated Automatically by an Evolutionary Algorithm (PANGAEA), discovers activation functions which improve performance over previous activation functions. PANGAEA produces different functions for Wide ResNet, ResNet, and Preactivation ResNet on the CIFAR-100 image classification task, demonstrating its ability to customize activation functions to architectures.

2 Related Work

Prior work in automatic activation function discovery includes that of Ramachandran et al. [24], who used reinforcement learning to design novel activation functions. They discovered multiple functions, but analyzed just one in depth: `Swish(x) = x · $\sigma(x)$` . Of the top eight functions discovered, only `Swish` and `max{x, $\sigma(x)$ }` consistently outperformed `ReLU` across multiple tasks, suggesting that improvements are possible but often task-specific.

Bingham et al. [3] used evolution to discover novel activation functions. While their functions had a fixed graph structure, PANGAEA utilizes a flexible search space that includes activation functions of arbitrary shape. PANGAEA also includes more powerful mutation operations, and a function parameterization approach that makes it possible to further refine functions through gradient descent.

Liu et al. [19] evolved normalization-activation layers. They searched for a computation graph that replaced both batch normalization and `ReLU` in multiple neural networks. They argued that the inherent nonlinearity of the discovered layers precluded the need for any explicit activation function. However, experiments in this paper show that carefully designed parametric activation functions can in fact be a powerful augmentation to existing deep learning models.

Finally, Basirat and Roth [2] used a genetic algorithm to discover task-specific piecewise activation functions. They showed that different functions are optimal for different tasks. However, the discovered activation functions did not outperform `ELiSH` and `HardELiSH`, two hand-designed activation functions proposed in the same paper [2]. The larger search space in PANGAEA affords evolution extra flexibility in designing activation functions, while the trainable parameters give customizability to the network itself, leading to consistent, significant improvement.

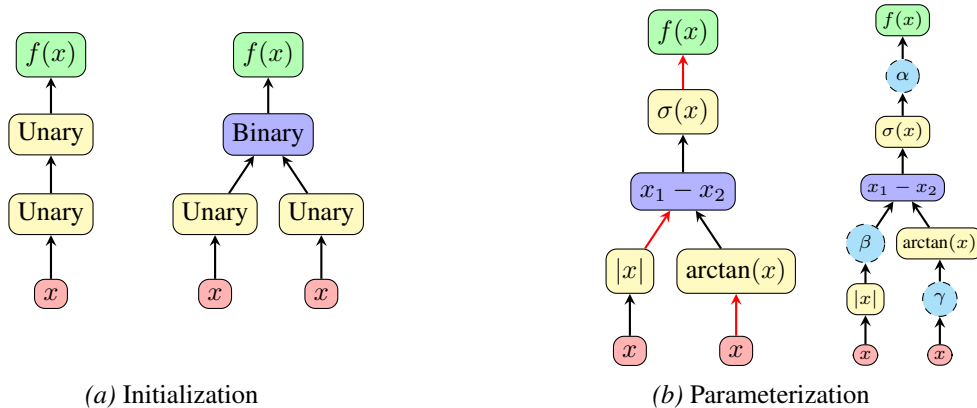


Figure 1: (a) Random activation function initialization. The initial population consists of random samples of two kinds of computation graphs, randomly initialized with the operators in Table 1. In this manner, the search starts with simple graphs and gradually expands to more complex forms. (b) Parameterization of activation functions. In this example, parameters are added to $k = 3$ random edges, yielding the parametric activation function $\alpha\sigma(\beta|x| - \arctan(\gamma x))$.

3 The PANGAEA Method

3.1 Representing and Searching for Activation Functions

Activation functions are represented as computation graphs in which each node is a unary or a binary operator. The list of possible operators is given in Table 1. The activation functions are implemented in TensorFlow [1], and safe operator implementations are chosen when possible (e.g. the binary operator x_1/x_2 is implemented as `tf.math.divide_no_nan`, which returns 0 if $x_2 = 0$). The unary and binary operators in Table 1 were chosen to create a large and expressive search space containing activation functions that are unlikely to be discovered by hand. Operators that are periodic (e.g. $\sin(x)$) and operators that contain repeated asymptotes were not included; in preliminary experiments they often caused training instability. All of the operators have domain \mathbb{R} , making it possible to compose them arbitrarily.

Evolution begins with an initial population of P random activation functions. Each function is either of the form $f(x) = \text{unary1}(\text{unary2}(x))$ or $f(x) = \text{binary}(\text{unary1}(x), \text{unary2}(x))$, as shown in Figure 1a. Both forms are equally likely, and the unary and binary operators are also selected uniformly at random. Previous work has suggested that it is difficult to discover high-performing activation functions that have complicated computation graphs [3]. The computation graphs in Figure 1 thus represent the simplest non-trivial computation graphs with and without a binary operator.

During evolution, all ReLU activation functions in a given neural network are replaced with a candidate activation function. No other changes to the network or training setup are made. The network is trained on the dataset, and the activation function is assigned a fitness score equal to the network’s accuracy on the *validation* set.

Given a parent activation function (Figure 2a), a child activation function is created by applying one of four possible mutations. Other possible evolutionary operators like crossover are not used in this paper. All mutations are equally likely with two special cases. If a remove mutation is selected for an activation function with just one node, a change mutation is applied instead. Additionally, if an activation function with greater than seven nodes is selected for mutation, the mutation is a remove mutation. This is done to control bloat.

Insert In an insert mutation, one operator in the search space is selected uniformly at random. This operator is placed on a random edge of a parent activation function graph. In Figure 2b, the unary operator $\text{Swish}(x)$ is inserted at the edge connecting the output of $\tanh(x)$ to the input of $x_1 + x_2$. After mutating, the parent activation function $(\tanh(x) + |\text{erf}(x)|)^2$ produces the child activation

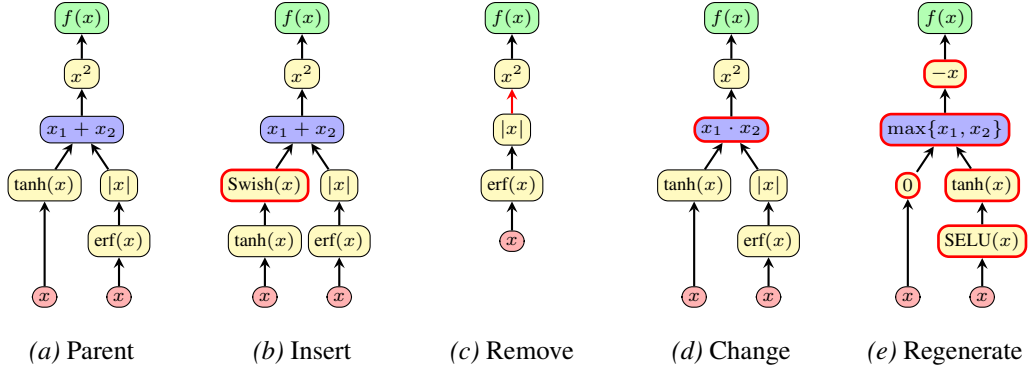


Figure 2: Evolutionary operations on activation functions. In an ‘Insert’ mutation, a new operator is inserted in one of the edges of the computation graph, like the Swish(x) in (b). In a ‘Remove’ mutation, a node in the computation graph is deleted, like the addition in (c). In a ‘Change’ mutation, an operator at a node is replaced with another, like addition with multiplication in (d). These first three mutations are useful in refining the function locally. In contrast, in a ‘Regenerate’ mutation (e), every operator in the graph is replaced by a random operator, thus increasing exploration.

function $(\text{Swish}(\tanh(x)) + |\text{erf}(x)|)^2$. If a binary operator is randomly chosen for the insertion, the incoming input value is assigned to the variable x_1 . If the operator is addition or subtraction, the input to x_2 is set to 0. If the operator is multiplication, division, or exponentiation, the input to x_2 is set to 1. Finally, if the operator is the maximum or minimum operator, the input to x_2 is a copy of the input to x_1 . When a binary operator is inserted into a computation graph, the activation function computed remains unchanged. However, the structure of the computation graph is modified and can be further altered by mutations in the future.

Remove In a remove mutation, one node is selected uniformly at random and deleted. The node’s input is rewired to its output. If the removed node is binary, one of the two inputs is chosen at random and is deleted. The other input is kept. In Figure 2c, the addition operator is removed from the parent activation function. The two inputs to addition, $\tanh(x)$ and $|\text{erf}(x)|$, cannot both be kept. By chance, $\tanh(x)$ is discarded, resulting in the child activation function $|\text{erf}(x)|^2$.

Change To perform a change mutation, one node in the computation graph is selected at random and replaced with another operator from the search space, also uniformly at random. Unary operators are always replaced with unary operators, and binary operators with binary operators. Figure 2d shows how changing addition to multiplication produces the activation function $(\tanh(x) \cdot |\text{erf}(x)|)^2$.

Regenerate In a regenerate mutation, every operator in the computation graph is replaced with another operator from the search space. Similar to change mutations, unary operators are replaced with unary operators, and binary operators with binary operators. Although every node in the graph is changed, the overall structure of the computation graph remains the same. Regenerate mutations are useful for increasing exploration, and are similar in principle to burst mutation and delta coding [8, 28]. Figure 2e shows the child activation function $-\max\{0, \tanh(\text{SELU}(x))\}$, which is substantially different from the parent activation function in Figure 2a.

3.2 Parameterization of Activation Functions

After mutation (or random initialization), activation functions are parameterized (Figure 1b). A value $k \in \{0, 1, 2, 3\}$ is chosen uniformly at random, and k edges of the activation function graph are randomly selected. Multiplicative per-channel parameters are inserted at these edges and initialized to one. Whereas evolution is well suited for discovering the general form of the activation function in a discrete, structured search space, parameterization makes it possible to fine-tune the function using gradient descent.

The function parameters are updated at every epoch during gradient descent, resulting in different activation functions in different stages of training. Since the parameters are per-channel, the process

creates different activation functions at different locations in the neural network. Thus, parameterization gives neural networks additional flexibility to customize activation functions, leading to significant increases in accuracy.

3.3 Evolutionary Process

Activation functions are discovered by regularized evolution [25]. Initially, P random activation functions are created, parameterized, and assigned fitness scores. To generate a new function, S activation functions are sampled with replacement from the current population. The function with the highest validation accuracy serves as the parent, and is mutated to create a child activation function. This function is parameterized and assigned a fitness score. The new function is then added to the population, and the oldest activation function in the population is removed, ensuring the population is always of size P . This process continues until C activation functions have been evaluated in total, and the top activation functions over the history of the search are returned as a result.

Any activation function that achieves validation accuracy less than a threshold V is discarded. These activation functions are not added to the population, but they do count towards the total number C of activation functions evaluated for each architecture. This quality control mechanism allows evolution to focus only on the most promising candidates.

To save computational resources during evolution, each activation function is evaluated by training a neural network for 100 epochs using a compressed learning rate schedule (Appendix A). After evolution is complete, the top 10 activation functions from the entire search are reranked. Each function receives an adjusted fitness score equal to the average *validation* accuracy from two independent 200-epoch training runs using the original learning rate schedule. The top three activation functions after reranking proceed to the final testing experiments.

During evolution, it is possible that some activation functions achieve unusually high validation accuracy by chance. It is also likely that the 100-epoch compressed learning rate schedule has a minor effect on which activation functions are optimal compared to a full 200-epoch learning rate schedule. Reranking thus serves two purposes. Full training eliminates any possible bias from the compressed learning rate schedule, and averaging two such runs reduces the impact of activation functions that achieved high accuracy due to chance.

4 Dataset and Architectures

The experiments in this paper use the CIFAR-100 image classification dataset [17]. This dataset is a more difficult version of the popular CIFAR-10 dataset, with 100 object categories instead of 10. Fifty images from each class were randomly selected from the training set to create a balanced validation set, resulting in a training/validation/test split of 45K/5K/10K images.

To demonstrate that PANGAEA can discover effective activation functions in different settings, it is evaluated with three different neural network architectures. In each case, the architectures were implemented in TensorFlow [1], mirroring the original authors' training setup as closely as possible. The full implementation details for each architecture are included in Appendix A.

Wide Residual Network (WRN-10-4) The first architecture is a wide residual network of depth 10 and widening factor four (WRN-10-4) [30]. Wide residual networks provide an interesting comparison because they are shallower and wider than many other popular architectures, while still achieving impressive results. WRN-10-4 was chosen because its accuracy is competitive with other architectures on CIFAR-100, yet it has a relatively low number of parameters, making it fast to train.

Residual Network (ResNet-v1-56) A residual network of depth 56 (ResNet-v1-56) [11] provides an important contrast to WRN-10-4. It is significantly deeper and has a slightly different training setup, which may have an effect on the performance of different activation functions.

Preactivation Residual Network (ResNet-v2-56) A preactivation residual network of depth 56 (ResNet-v2-56) [12] has identical depth to ResNet-v1-56, but is a fundamentally different architecture. Activation functions are not part of the skip connections, as is the case in ResNet-v1-56. Since information does not have to pass through an activation function, this structure makes it easier to train

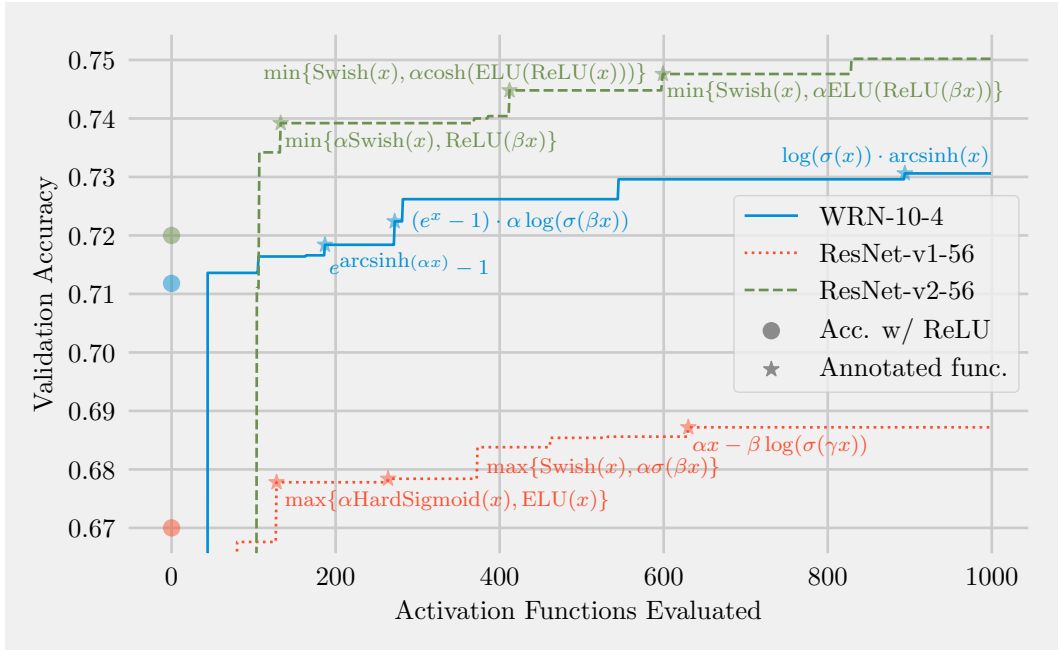


Figure 3: Progress of PANGAEA with the three architectures. Each PANGAEA run uses a different architecture as identified by color. Evolution quickly discovers activation functions that outperform ReLU (shown as a colored circle at $x = 0$), and continues to make progress throughout the experiment. The plots show the highest validation accuracy of all activation functions evaluated so far. Interesting activation functions discovered are identified with a star and annotated. The accuracy reported is on the validation set after 100 epochs of training. The improvements over ReLU are meaningful, but the values themselves are not directly comparable to the results in Table 2, which lists accuracy on the test set after 200 epochs of training.

very deep architectures. PANGAEA should exploit this structure and discover different activation functions for ResNet-v2-56 and ResNet-v1-56.

5 Results

Three separate evolution experiments were run to discover novel activation functions for the three architectures. Evolutionary parameters $P = 64$, $S = 16$, $C = 1,000$, and $V = 0.2$ were used since they were found to work well in preliminary experiments. Figure 3 visualizes the progress of the three runs. For all three architectures, PANGAEA quickly discovers activation functions that outperform ReLU. It continues to make progress, gradually discovering better activation functions. Notably, evolution makes steady progress throughout the run and does not plateau during the time allotted for the experiment. Each run took approximately 2,000 GPU hours on GeForce GTX 1080 GPUs (Appendix B).

Table 2 shows the final test accuracy for the top activation functions discovered by PANGAEA. For comparison, each architecture was also trained with 12 previously proposed activation functions. These 12 functions are diverse and constitute a powerful baseline. Seven of the 12 functions outperform ReLU with at least one network architecture. Only ELU, GELU, and Swish outperform ReLU across all three architectures; however, the improvements are marginal. PANGAEA, on the other hand, consistently discovers new parametric activation functions for each architecture which significantly improve performance. In fact, PANGAEA discovered the best activation function for ResNet-v2-56, the top two activation functions for ResNet-v1-56, and three activation functions that outperformed all other evaluated activation functions for WRN-10-4.

Many of the top discovered activation functions are compositions of multiple unary operators. These functions do not exist in the core unit search space of Ramachandran et al. [24], which requires binary

Table 2: CIFAR-100 test set accuracy. With previously proposed activation functions, performance gains relative to ReLU are inconsistent or marginal. In contrast, PANGAEA consistently discovered specialized functions that lead to significant improvements. Results that outperform ReLU are highlighted in green, while those that underperform it are in red. The top accuracy for each architecture is in bold. Results for previously proposed activation functions are based on a single run; results for ReLU and the evolved activation functions are shown as a median of five runs, with mean \pm standard deviation in parentheses.

	WRN-10-4	ResNet-v1-56	ResNet-v2-56
ReLU	71.23 (71.09 \pm 0.36)	69.20 (69.24 \pm 0.71)	74.06 (74.05 \pm 0.23)
$\log(\sigma(\alpha x)) \cdot \beta \text{arcsinh}(x)$	73.07 (72.97 \pm 0.31)		
$\log(\sigma(\alpha x)) \cdot \text{arcsinh}(x)$	72.89 (72.88 \pm 0.31)		
$-\text{Swish}(\text{Swish}(x))$	72.35 (72.27 \pm 0.29)		
$\alpha x - \beta \log(\sigma(\gamma x))$		70.55 (70.53 \pm 0.20)	
$\alpha x - \log(\sigma(\beta x))$		70.11 (70.14 \pm 0.67)	
$\max\{\text{Swish}(x), 0\}$		68.80 (68.87 \pm 0.41)	
Softplus(ELU(x))			75.23 (75.27 \pm 0.21)
SELU(Swish(x))			74.78 (74.77 \pm 0.25)
$\min\{\log(\sigma(x)), \alpha \log(\sigma(\beta x))\}$			74.75 (74.92 \pm 0.27)
ELiSH [2]	01.00	01.00	74.82
ELU [4]	71.83	69.37	74.85
GELU [13]	71.28	70.03	74.33
HardSigmoid	54.44	23.32	63.90
Leaky ReLU [20]	71.84	69.38	73.84
Mish [21]	71.89	68.82	75.04
SELU [16]	69.86	68.48	73.76
sigmoid	56.81	36.45	65.25
Softplus	71.82	69.10	74.54
Softsign	56.77	59.82	68.90
Swish [24, 6]	71.71	69.34	74.28
tanh	58.25	63.18	69.77

operators. They also do not exist in the S_1 or S_2 search spaces proposed by Bingham et al. [3], which are too shallow. The design of the search space is therefore as important as the search algorithm itself. Previous search spaces that rely on repeated fixed building blocks only have limited representational power. In contrast, PANGAEA utilizes a flexible search space that can represent activation functions in an arbitrary computation graph. The advantage of this approach is evident in the results.

Figure 4 shows examples of parametric activation functions discovered by PANGAEA. As training progresses, gradient descent makes small adjustments to the function parameters α , β , and γ , resulting in activation functions that change over time (Figure 4a). This result suggests that it is advantageous to have one activation function in the early stages of training when the network learns rapidly, and a different activation function in the later stages of training, when the network is focused on fine-tuning. The parameters α , β , and γ are also learned separately for the different channels, resulting in activation functions that vary with location in a neural network (Figure 4b). Functions in deep layers (those near the output) are more nonlinear than those in shallow layers (those closer to the input), possibly contrasting the need to form regularized embeddings with the need to form categorizations. In this manner, PANGAEA customizes the activation functions to both time and space for each architecture.

6 Future Work

It is difficult to select an appropriate activation function for a given architecture and task because the activation function, the topology of the network, and the general training setup interact in complex ways. It is therefore especially promising that PANGAEA was able to discover activation functions that significantly outperformed the baseline, since the architectures and training setup were standard and developed with ReLU. A most compelling research direction is to optimize the architecture and training setup together with the activation functions.

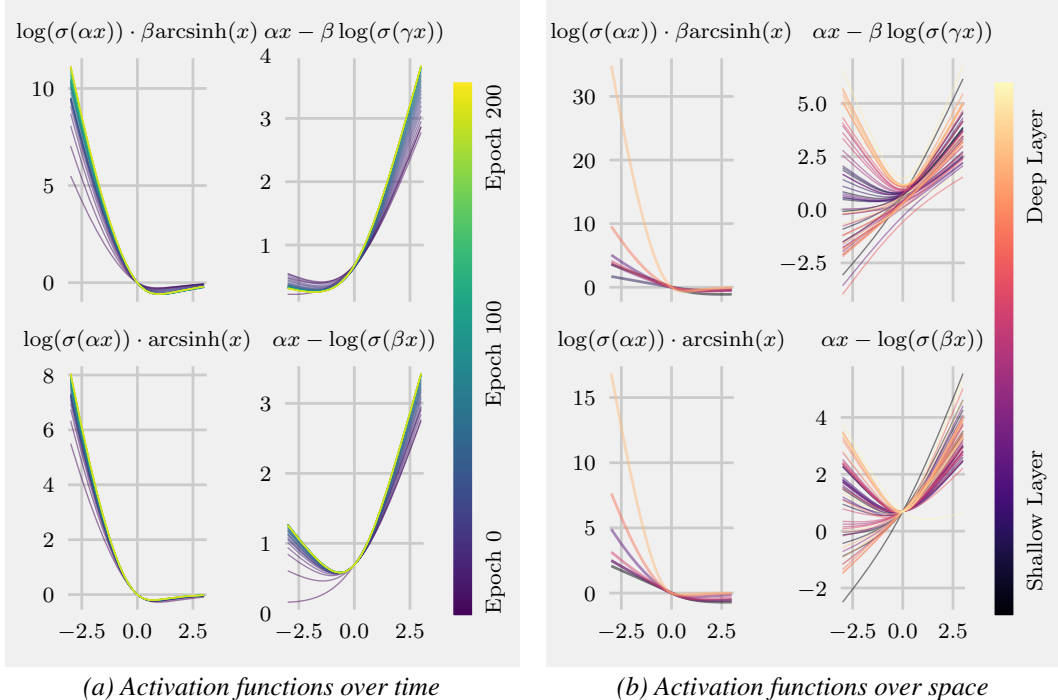


Figure 4: Adaptation of parametric activation functions over time and space. (a) The parameters change during training, resulting in different activation functions in the early and late stages. The plots were created by averaging the values of α , β , and γ across the entire network at different training epochs. (b) The parameters are updated separately in each channel, inducing different activation functions at different locations of a neural network. The plots were created by averaging α , β , and γ at each layer of the network after the completion of training. Thus, PANGAEA customizes the activation functions to both time and space for each architecture, improving performance.

More specifically, there has been significant recent research in automatically discovering the architecture of neural networks through gradient-based, reinforcement learning, or neuroevolutionary methods [7, 29, 25]. In related work, evolution was used to discover novel loss functions automatically [9, 10, 18], outperforming the standard cross entropy loss. In the future, it may be possible to optimize many of these aspects of neural network design jointly. Just as new activation functions improve the accuracy of existing network architectures, it is likely that different architectures will be discovered when the activation function is not ReLU. One such example is EfficientNet [26], which set a new state-of-the-art accuracy for ImageNet [5] using the Swish activation function [24, 6]. Coevolution of activation functions, topologies, loss functions, and possibly other aspects of neural network design could allow taking advantage of interactions between them, leading to further improvements in the future.

7 Conclusion

This paper introduced PANGAEA, a technique for automatically designing novel, high-performing, parametric activation functions. PANGAEA builds a synergy of two different optimization processes: evolutionary population-based search for the general form, and gradient-descent-based fine tuning of the parameters of the activation function. Compared to previous studies, the search space is extended to include deeper and more complex functional forms, including ones unlikely to be discovered by humans. The parameters are adapted during training and are different in different locations of the architecture, thereby adapting the activation functions for different stages of learning and computational needs within the network. PANGAEA consistently discovers activation functions that result in substantial improvements for all three architectures considered. It is a promising step towards fully automatic configuration of neural networks.

Broader Impact

This paper presents an algorithm to automatically discover parametric activation functions which increase accuracy for different neural networks. PANGAEA has the potential to be used as an automated optimization step in machine learning engineering. Increasing the accuracy and reliability of machine learning systems in production around the world with minimal additional human labor would be a significant positive impact.

The computational resources required to run the experiments in this paper should not be understated. It is likely that with even more compute power (i.e. if evolution evaluated more activation functions, or if the same experiments were applied to larger neural networks) that even better results could be achieved. A potential negative impact of this work is that it could exacerbate existing disparities in machine learning research. Those with access to large amounts of compute power have the greatest potential to benefit from this work.

Acknowledgments and Disclosure of Funding

The authors acknowledge the Texas Advanced Computing Center (TACC) at The University of Texas at Austin for providing HPC resources that have contributed to the research results reported within this paper.

References

- [1] M. Abadi, P. Barham, J. Chen, Z. Chen, A. Davis, J. Dean, M. Devin, S. Ghemawat, G. Irving, M. Isard, et al. Tensorflow: A system for large-scale machine learning. In *12th {USENIX} Symposium on Operating Systems Design and Implementation ({OSDI} 16)*, pages 265–283, 2016.
- [2] M. Basirat and P. M. Roth. The quest for the golden activation function. *arXiv preprint arXiv:1808.00783*, 2018.
- [3] G. Bingham, W. Macke, and R. Miikkulainen. Evolutionary optimization of deep learning activation functions. In *Genetic and Evolutionary Computation Conference (GECCO '20), July 8–12, 2020, Cancún, Mexico*, 2020.
- [4] D.-A. Clevert, T. Unterthiner, and S. Hochreiter. Fast and accurate deep network learning by exponential linear units (elus). *CoRR*, abs/1511.07289, 2015.
- [5] J. Deng, W. Dong, R. Socher, L.-J. Li, K. Li, and L. Fei-Fei. Imagenet: A large-scale hierarchical image database. In *2009 IEEE conference on computer vision and pattern recognition*, pages 248–255. Ieee, 2009.
- [6] S. Elfving, E. Uchibe, and K. Doya. Sigmoid-weighted linear units for neural network function approximation in reinforcement learning. *Neural Networks*, 107:3–11, 2018.
- [7] T. Elsken, J. H. Metzen, and F. Hutter. Neural architecture search: A survey. *Journal of Machine Learning Research*, 20(55):1–21, 2019.
- [8] F. Gomez and R. Miikkulainen. Active guidance for a finless rocket using neuroevolution. In *Proceedings of the Genetic and Evolutionary Computation Conference*, pages 2084–2095, 2003.
- [9] S. Gonzalez and R. Miikkulainen. Improved training speed, accuracy, and data utilization through loss function optimization. *arXiv preprint arXiv:1905.11528*, 2019.
- [10] S. Gonzalez and R. Miikkulainen. Evolving loss functions with multivariate taylor polynomial parameterizations. *arXiv preprint arXiv:2002.00059*, 2020.
- [11] K. He, X. Zhang, S. Ren, and J. Sun. Deep residual learning for image recognition. In *Proceedings of the IEEE conference on computer vision and pattern recognition*, pages 770–778, 2016.
- [12] K. He, X. Zhang, S. Ren, and J. Sun. Identity mappings in deep residual networks. In *European conference on computer vision*, pages 630–645. Springer, 2016.
- [13] D. Hendrycks and K. Gimpel. Gaussian error linear units (gelus). *arXiv preprint arXiv:1606.08415*, 2016.
- [14] G. E. Hinton, N. Srivastava, A. Krizhevsky, I. Sutskever, and R. R. Salakhutdinov. Improving neural networks by preventing co-adaptation of feature detectors. *arXiv preprint arXiv:1207.0580*, 2012.

- [15] S. Ioffe and C. Szegedy. Batch normalization: Accelerating deep network training by reducing internal covariate shift. In *International Conference on Machine Learning*, pages 448–456, 2015.
- [16] G. Klambauer, T. Unterthiner, A. Mayr, and S. Hochreiter. Self-normalizing neural networks. In *Advances in neural information processing systems*, pages 971–980, 2017.
- [17] A. Krizhevsky, G. Hinton, et al. Learning multiple layers of features from tiny images. 2009.
- [18] J. Liang, S. Gonzalez, and R. Miikkulainen. Population-based training for loss function optimization. *arXiv preprint arXiv:2002.04225*, 2020.
- [19] H. Liu, A. Brock, K. Simonyan, and Q. V. Le. Evolving normalization-activation layers. *arXiv preprint arXiv:2004.02967*, 2020.
- [20] A. L. Maas, A. Y. Hannun, and A. Y. Ng. Rectifier nonlinearities improve neural network acoustic models. In *Proc. icml*, volume 30, page 3, 2013.
- [21] D. Misra. Mish: A self regularized non-monotonic neural activation function. *arXiv preprint arXiv:1908.08681*, 2019.
- [22] V. Nair and G. E. Hinton. Rectified linear units improve restricted boltzmann machines. In *Proceedings of the 27th international conference on machine learning (ICML-10)*, pages 807–814, 2010.
- [23] C. Nwankpa, W. Ijomah, A. Gachagan, and S. Marshall. Activation functions: Comparison of trends in practice and research for deep learning. *arXiv preprint arXiv:1811.03378*, 2018.
- [24] P. Ramachandran, B. Zoph, and Q. V. Le. Searching for activation functions. In *6th International Conference on Learning Representations, ICLR 2018, Vancouver, BC, Canada, April 30 - May 3, 2018, Workshop Track Proceedings*, 2018.
- [25] E. Real, A. Aggarwal, Y. Huang, and Q. V. Le. Regularized evolution for image classifier architecture search. In *Proceedings of the aaii conference on artificial intelligence*, volume 33, pages 4780–4789, 2019.
- [26] M. Tan and Q. Le. Efficientnet: Rethinking model scaling for convolutional neural networks. In *International Conference on Machine Learning*, pages 6105–6114, 2019.
- [27] D. Thain, T. Tannenbaum, and M. Livny. Distributed computing in practice: the condor experience. *Concurrency and computation: practice and experience*, 17(2-4):323–356, 2005.
- [28] D. Whitley, K. Mathias, and P. Fitzhorn. Delta-Coding: An iterative search strategy for genetic algorithms. pages 77–84.
- [29] M. Wistuba, A. Rawat, and T. Pedapati. A survey on neural architecture search. *arXiv preprint arXiv:1905.01392*, 2019.
- [30] S. Zagoruyko and N. Komodakis. Wide residual networks. *arXiv preprint arXiv:1605.07146*, 2016.

A Training Details

Wide Residual Network (WRN-10-4) When measuring final performance after evolution, the standard WRN setup is used; all ReLU activations in WRN-10-4 are replaced with the evolved activation function, but no other changes to the architecture are made. The network is optimized using stochastic gradient descent with Nesterov momentum 0.9. The network is trained for 200 epochs; the initial learning rate is 0.1, and it is decreased by a factor of 0.2 after epochs 60, 120, and 160. Dropout probability is set to 0.3, and L2 regularization of 0.0005 is applied to the weights. Data augmentation includes featurewise center, featurewise standard deviation normalization, horizontal flip, and random 32×32 crops of images padded with four pixels on all sides. This setup was chosen to mirror the original WRN setup [30] as closely as possible.

During evolution of activation functions, the training is compressed to save time. The network is trained for only 100 epochs; the learning rate begins at 0.1 and is decreased by a factor of 0.2 after epochs 30, 60, and 80. Empirically, the accuracy achieved by this shorter schedule is sufficient to guide evolution; the computational cost saved by halving the time required to evaluate an activation function can then be used to search for additional activation functions.

Residual Network (ResNet-v1-56) As with WRN-10-4, when measuring final performance with ResNet-v1-56, the only change to the architecture is replacing the ReLU activations with an evolved activation function. The network is optimized with stochastic gradient descent and momentum 0.9. Dropout is not used, and L2 regularization of 0.0001 is applied to the weights. In the original ResNet experiments [11], an initial learning rate of 0.01 was used for 400 iterations before increasing it to 0.1, and further decreasing it by a factor of 0.1 after 32K and 48K iterations. An iteration represents a single forward and backward pass over one training batch, while an epoch consists of training over the entire training dataset. In this paper, the learning rate schedule is implemented by beginning with a learning rate of 0.01 for one epoch, increasing it to 0.1, and then decreasing it by a factor of 0.1 after epochs 91 and 137. (For example, (48K iterations / 45K training images) * batch size of $128 \approx 137$.) The network is trained for 200 epochs in total. The data augmentation includes random horizontal flip and random 32×32 crops of images padded with four pixels on all sides, as in the original setup [11].

When evolving activation functions for ResNet-v1-56, the learning rate schedule is again compressed. The network is trained for 100 epochs; the initial warmup learning rate of 0.01 still lasts one epoch, the learning rate increases to 0.1, and then decreases by a factor of 0.1 after epochs 46 and 68. When evolving activation functions, their relative performance is more important than the absolute accuracies they achieve. The shorter training schedule is therefore a cost-efficient way of discovering high-performing activation functions.

Preactivation Residual Network (ResNet-v2-56) The full training setup, data augmentation, and compressed learning rate schedule used during evolution for ResNet-v2-56 are all identical to those for ResNet-v1-56 with one exception. With ResNet-v2-56, it is not necessary to warm up training with an initial learning rate of 0.01 [12], so this step is skipped.

B Implementation and Compute Requirements

High-performance computing in two clusters is utilized for the experiments. One cluster uses HTCondor [27] for scheduling jobs, while the other uses the Slurm workload manager. Training is executed on GeForce GTX 1080 GPUs on both clusters. When a job begins executing, a parent activation function is selected by sampling $S = 16$ functions from the $P = 64$ most recently evaluated activation functions. This is a minor difference from the original regularized evolution [25], which is based on a strict sliding window of size P . This approach may give extra influence to some activation functions, depending on how quickly or slowly jobs are executed in each of the clusters. In practice the method is highly effective; it allows evolution to progress quickly by taking advantage of extra compute when demand on the clusters is low.

It is difficult to know ahead of time how computationally expensive the evolutionary search will be. Some activation functions immediately result in an undefined loss, causing training to end. In that case only a few seconds have been spent and another activation function can immediately be evaluated. Other activation functions train successfully, but their complicated expressions result in slightly longer-than-usual training times. In these experiments, evolution for WRN-10-4 took 2,314 GPU hours, evolution for ResNet-v1-56 took 1,594 GPU hours, and evolution for ResNet-v2-56 took 2,175 GPU hours. These numbers do not include costs for reranking and repeated runs in the final experiments. Although substantial, the computational cost is negligible compared to the cost in human labor in designing activation functions. Evolution of parametric activation functions requires minimal manual setup and delivers automatic improvements in accuracy.